Exploratory Topological Study of the Laplacian of the Electronic Charge Density in *n*-Butonium Cations

R. M. Lobayan,[§] G. L. Sosa,[§] A. H. Jubert,*[,#] and N. M. Peruchena[§]

Area de Química Física, Facultad de Ciencias Exactas y Naturales y Agrimensura, UNNE, Avda. Libertad 5460, (3400) Corrientes, Argentina, and CEQUINOR (CONICET, UNLP), Departamento de Química, Facultad de Ciencias Exactas and Facultad de Ingeniería, UNLP, C.C. 962, Calle 47 y 115 (1900) La Plata, Argentina

Received: January 20, 2004; In Final Form: March 11, 2004

In this work we present a systematic HF/6-311++G** study of the topology of the Laplacian of the electronic density for 11 carbocations, generated upon the insertion of a proton into the C−C or C−H bonds during the protonation of *n*-butane, two 2-*C*-*n*-butonium cations, three 1-*C*-*n*-butonium cations, three 2-*H*-*n*-butonium cations, and three 1-*H*-*n*-butonium cations. This is the continuation of previous work where the charge density topology of *n*-butoniums at the same level of approach was studied. The Laplacian charge concentration critical points at each valence shell of the carbon atoms are analyzed, and also both the charge concentration and the charge depletion critical points closer to the hydrogen atoms are studied. Our exploratory analysis shows that the study of the Laplacian topology of the electronic density can be used as a suitable tool in order to quantify the displacement effects of the electronic density through the sigma bonds, the delocalization of the positive charge (in our case introduced into the system by a proton), and the degree of electronic deficiency of the carbon atom. It is demonstrated here how these facts allow us to understand the stability order found in the studied carbocationic species: 2-*C*-*n*-butoniums > 1-*C*-*n*-butoniums > 2-*H*-*n*-butoniums > 1-*H*-*n*-butoniums.

Introduction

Carbonium ions are important species involved in acid-catalyzed alkane transformations. They are formed by the insertion of a proton into C−C or C−H bonds and present one characteristic three-center-two-electron bonds (3c-2e). The methonium[1] (CH_5^+) and ethonium[2] ($C_2H_7^+$) ions are the smallest members of this family and have already been observed in the gas phase by spectroscopic methods.[3,4] They have also been mostly studied by theoretical methods. The use of ab initio calculations, particularly those including electron correlations effects, has proven to provide excellent predictions for the equilibrium energy and geometry of these carbocations.

For the $C_2H_7^+$ cation, theoretical calculations[5,6] reveal *C*-ethonium, hypothetically formed through the protonation in the C−C bond of ethane, as the lowest energy species. More recently[6] it has been demonstrated that the $C_2H_7^+$ ion presents three isomeric forms at low temperature: one form protonated in the C−C bond, one form protonated in the C−H bond, and one form that results from the interaction between a H_2 molecule and the $C_2H_5^+$ ion, the latter corresponding to a van der Waals complex. The most stable structure is the *C*-ethonium ion, followed by the *H*-ethonium ion and the complex $C_2H_5^+ \cdot H_2$.

Esteves et al. have performed ab initio calculations for the proponium,[7] isobutonium,[8] and the *n*-butonium[9a,b] cations, at the perturbational second- and fourth-order Møller−Plesset levels of theory. For *i*-$C_4H_{11}^+$, protonated isobutane, the calculations indicated that the van der Waals complexes between *tert*-butyl carbenium ion and hydrogen and isopropyl carbenium ion and methane have a lower energy than the carbonium ions themselves. Indeed, additional calculations[9b] revealed that decomposition of 2-*H*-isobutonium, hypothetically formed through the protonation of the tertiary C−H bond of isobutane, and *C*-isobutonium, formed upon protonation of the C−C bond of isobutane, to the respective van der Waals complexes occurs with low or no activation energy. A similar conclusion was found by Collins and O'Malley using DFT calculations.[10]

SCHEME 1: Hypothetical Protonation over Nonequivalent Bonds in *n*-Butane, Leading to the Different *n*-Butonium Cations

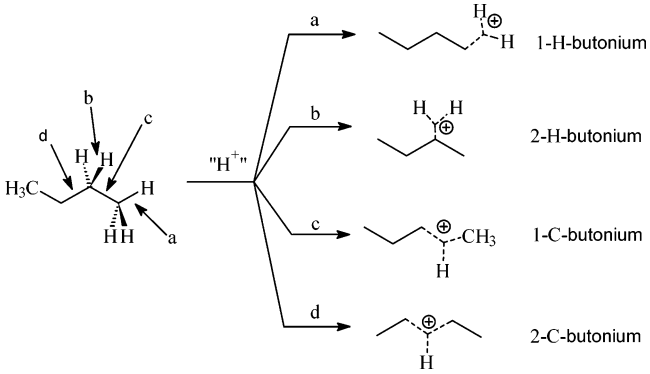

Protonation of *n*-butane can take place at the primary or secondary C−H bonds and at two different types of C−C bonds, external or internal, to form different isomeric structures of *n*-butonium cations, as shown in Scheme 1. The stability of these carbonium ions decreases in the order

2-*C*-*n*-butonium > 1-*C*-*n*-butonium > 2-*H*-*n*-butonium > 1-*H*-*n*-butonium

Taking into consideration that the *i*-$C_4H_{11}^+$ cations are isomeric to the *n*-$C_4H_{11}^+$ cations, a direct comparison of energy

§ UNNE.
# UNLP.

10.1021/jp049717p CCC: $27.50
Published on Web 04/20/2004

SCHEME 2: Representation of the 3c-2e Bond in *H*-Carbonium and *C*-Carbonium Ions by Valence Bond (VB) Resonance Structures

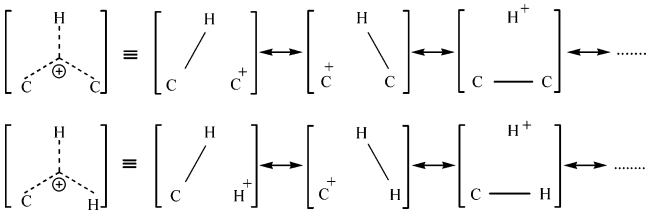

among them is possible. Consequently, Esteves et al. have proposed the following σ-basicity scale[11] on the basis of the relative stability of the carbocations:

$$\text{C}-\text{C} > \text{tert-C}-\text{H} > \text{sec-C}-\text{H} > \text{prim C}-\text{H} > \text{CH}_4$$

This scale differs slightly from the one proposed by Olah,[12] related to the reactivity of the σ-bond. The σ-reactivity scale is

$$\text{tert-C}-\text{H} > \text{C}-\text{C} > \text{sec-C}-\text{H} > \text{prim C}-\text{H} > \text{CH}_4$$

However, it must be taken into consideration that the Esteves' scale is related to the thermodynamics of the protonation of the σ-bond, reflecting the basicity of the bonds.

In previous works,[13,14] we have analyzed the topology of the distribution of the charge density in protonated species of *n*-butane and *i*-butane and their van der Waals complexes; this analysis has been used in order to establish a relationship among the parameters that determine the stability order found for the different species and relate them with the carbonium ion's structure. We found that a better understanding of the relative stability of *n*-butane and *i*-butane is obtained when the topological properties at the bond critical points on the distribution of the electronic charge density in the 3c-2e bonds are considered. A 3c-2e bond of the C−H*−H* type is found in all of the *H*-butonium cations, and also a 3c-2e bond of the C−H*−C type is found in all of the *C*-butonium cations. These studies showed that the stability of the protonated species, both *C*-*n*-butonium and *H*-*n*-butonium cations, depends fundamentally on the way in which the charge of the cation is delocalized around the 3c-2e bonds. In these works we concluded that, in *H*-*n*-butonium cations, the stabilization degree is related to an increase of the electronic density between the H* atoms, at the H*−H* bond, and to a decrease of the density between the H* and C atoms involved in the three-center bond. These facts are accompanied by a shortening of the H*−H* and a lengthening of the C−H* distances and a decrease of the H*−C−H* angle. This explains that a higher stability is associated with a more stable carbenium ion interacting with the H_2 moiety. In addition, these findings also reveal that the higher stability corresponds to the more substituted carbenium moiety, (i.e., $C_{sec} > C_{prim}$) in the resonance structures (Scheme 2).

After analyzing the topology of the distribution of the charge density in all *C*-butonium cations, we have found indicators of the delocalization of electron charge density on the atoms involved in the three-center bond and in the remaining fragments. This delocalization of the density on the C−H* bonds and neighboring C−X bonds (with X = C, H) is higher in $C_{sec}-H^*-C_{sec}$ than in $C_{prim}-H^*-C_{sec}$ in *C*-*n*-butonium cations but lower than the delocalization that occurs in $C_{tert}-H^*-C_{met}$ at the *C*-*i*-butonium cation. Thus, from topological considerations, the stability order is

$$C_{tertiary} > C_{secondary} > C_{primary}$$

These results agree with the idea that these species achieve their stabilization through the distribution of the positive charge of the proton onto the sigma bonds.

A deep knowledge of the electronic structure of these carbocationic species is essential in order to understand the mechanisms that occur during the catalytic process in the transformation of hydrocarbons.

In this work we present the results derived from a study of the topology of the Laplacian distribution of the electronic charge density for the molecular species mentioned above, in order to investigate not only what occurs in the 3c-2e bonds but also the role of the neighboring bonds in the redistribution of the electronic charge density. This can be seen in the topology of the Laplacian distribution through the shifting of its critical points of concentration charge toward the electron deficient region at the 3c-2e bonds.

AIM Theory

The topological analysis derived from the theory of atoms in molecules (AIM), developed by Bader et al.[15,16] was extensively applied to study different chemical properties.[17−25] The analysis of the critical points (CP) of the Laplacian distribution of the electronic density has been demonstrated to be a potentially useful tool to study different significant chemical features, such as the structure and geometry of hydrogen-bonded complexes,[26] and to predict the sites of electrophilic and nucleophilic attack and their relative reactivities.[27−29] The CPs corresponding to the nonbonded charge concentrations were employed as sensitive probes of the differential delocalization/localization of the lone pairs.[30] The Laplacian function was applied to study the problems associated with the prediction and understanding of biochemical processes and catalysis phenomena[31−34] and provided a physical basis for the VSEPR (valence shell electronic pair repulsion) model.[35,36] The correspondence between the CPs of the Laplacian and the electron pairs in the VESPR model was the subject of recent studies,[37−42] and the full topology of the Laplacian in small molecules was also recently explored.[43,44]

It has to be remarked that the density is a physical property of the total system and not a model. Since 1960, the distribution of the electronic density charge, $\rho_{(r)}$, as a physical observable, has been determined experimentally by means of the diffraction of X-rays[45(a)]. Nevertheless, the study of molecules of medium size (20−30 atoms) with the use of conventional diffractometers and by means of a serial detection technique required periods of time as long as several weeks or even months. These difficulties meant that only qualitative results were obtained for molecules of larger size (i.e., proteins,[45(b)]). Although in the last few years several developments have improved this situation substantially (synchrotron radiation at low temperature and new and better area detectors[46]), the most refined results of $\rho_{(r)}$ required days. These difficulties are especially true in the field of carbocations due to their short life. The unstable nature of these species has prevented a detailed examination of their properties via experimental techniques. Thus, these restrictive experimental conditions demand that theoretical calculations be used to make valuable contributions.

The concentrations and depletions of charge at all the hydrogen atoms and the concentration of charge over all carbon atoms present in the *n*-butonium cations are analyzed in a systematic way. The determination of the (3, −3) and (3, +3) CPs on the H atoms, corresponding to local maxima and minima of the Laplacian distribution, and the (3, −3) CPs on the valence shell (valence shell, VS) of the carbon atoms, and the evaluation of the different topological parameters over them, allows us to

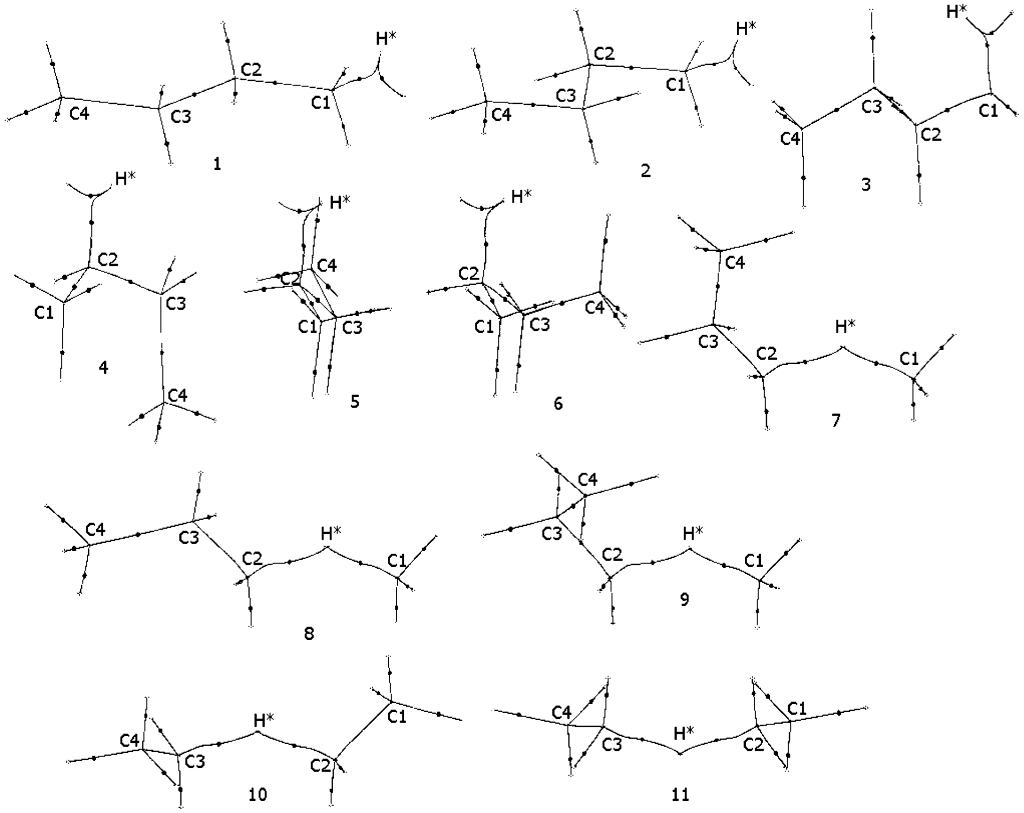

Figure 1. Molecular graphs of 1-*H*-*n*-butoniums (**1**, **2**, and **3**); 2-*H*-*n*-butoniums (**4**, **5**, and **6**); 1-*C*-*n*-butoniums (**7**, **8**, and **9**), and 2-*C*-*n*-butoniums (**10** and **11**).

visualize the changes that operate on the distribution of the electronic density, depending on the protonation site of the hydrocarbon. On the other hand, to date there is no systematic study of the Laplacian of the density of these carbocationic species that presents the singular feature of a three-center-two-electron bond (3c-2e).[12] Frequently, this methodology is employed to detect nucleophilic and electrophilic attack sites. In this work, it is also shown how other aspects of the Laplacian topology can be useful for obtaining deeper insights related to charge delocalization in sigma bonds. As stated above, this work is the continuation of previous work where the charge density topology of *n*-butoniums at the HF/6-311++G** level was studied,[14] and it corresponds to an exploratory study on the usefulness and applicability of the analysis of the Laplacian topology based principally in the charge concentration in CPs study.

Calculation Method and Analytical Details

The geometries of the different species were optimized at the MP2/(full)/6-31G** level,[9b] and the wave functions used for the topological analysis were obtained at the HF/6-311++G** level, as previously used for the *n*-butonium,[14] isobutonium,[13a] and proponium cations.[13b] Topological calculations preformed at the MP2/6-311++G** level showed no significant differences with results obtained at the HF/6-311++G** level.[13b] However, it is important to point out that in order to examine the effects of electron correlation, wave functions at the MP2/6-311++G** level have been used for the topological analysis in systems **10** and **11**, and we obtained similar results to those obtained at the HF level. All these calculations were performed using the Gaussian 98 package.[47]

The evaluation of the density and Laplacian distribution of the electronic charge density are accomplished by means of the AIMPAC package.[48]

Since the use of the topological concepts is well documented in the standard literature,[15,49] we only present here the key theoretical details which are needed for the discussion of the numerical results.

The Laplacian of ρ is defined by the equation

$$\nabla^2\rho = \partial^2\rho/\partial x^2 + \partial^2\rho/\partial y^2 + \partial^2\rho/\partial z^2$$

The relief map of the Laplacian function for the atomic system exhibits a shell of charge concentration and another one of charge depletion for each quantum shell. The outer quantum shell of an atom over $\nabla^2\rho < 0$ is called valence shell charge concentration (VSCC). For an isolated atom there is located a sphere where the valence electronic charge is maximally and uniformly concentrated. The VSCC loses its uniformity when the atom is within a chemical bond. The local maxima that are created provide a one-to-one mapping of the electron pairs of the Lewis and VSEPR model.[15,35,36]

Topologically, the extremes or critical points in the distribution of the Laplacian function of ρ are classified by their rank and signature in the same way as is done for the CPs in the charge density. The CPs of the Laplacian appear where $\nabla(\nabla^2\rho) = 0$, and the eigenvalues of the Hessian of $\nabla^2\rho$ indicate the principal curvatures of $\nabla\ ^2\rho$ in the CP. According to some authors,[43] it is convenient, for a more intuitive interpretation, to consider the $-\nabla^2\rho$ function. A (3, −3) CP corresponds to a local maximum in $-\nabla^2\rho$ (with $\nabla^2\rho < 0$) and indicates a local electronic charge concentration (CC), while a (3, +3) CP corresponds to a local minimum in $-\nabla^2\rho$ (with $\nabla^2\rho > 0$) and indicates a local depletion of the electronic charge (CD).

Results and Discussion

In Figure 1 we display the molecular graphs of the 11 carbocationic species that result from the protonation of the

TABLE 1: Topological Local Properties at the (3, −3) CPs of $-\nabla^2\rho_{(r_c)}$ in the Valence Shell of the Carbon Atoms in *n*-Butane and the 2-*C*-*n*-Butonium Cations[a]

	n-butane				**10**				**11**			
	$-\nabla^2\rho(r)$	r_c	λ_3	ϵ	$-\nabla^2\rho(r)$	r_c	λ_3	ϵ	$-\nabla^2\rho(r)$	r_c	λ_3	ϵ
					VS of C_1							
H	1.138	1.025	−12.470	0.0096	1.217	1.010	−14.572	0.0408	1.219	1.010	−14.627	0.0409
H	1.132	1.026	−12.294	0.0088	1.167	1.014	−13.893	0.0227	1.169	1.014	−13.909	0.0237
H	1.132	1.026	−12.294	0.0088	1.207	1.012	−14.289	0.0411	1.207	1.012	−14.287	0.0412
C_2	0.971	0.998	−17.390	0.0067	0.847	1.043	−10.418	0.0676	0.844	1.044	−10.335	0.0668
					VS of C_2							
C_1	0.962	1.000	−17.003	0.0090	1.263	0.953	−26.871	0.0769	1.264	0.953	−26.946	0.0767
H	1.138	1.025	−12.325	0.0101	1.377	0.980	−19.468	0.0744	1.364	0.981	−19.185	0.0722
H	1.138	1.025	−12.326	0.0109	1.420	0.977	−20.122	0.0833	1.417	0.978	−20.001	0.0819
H*, C_3	0.984	0.996	−17.615	0.0219								
					VS of C_3							
H*, C_2	0.984	0.996	−17.614	0.0219								
H	1.138	1.025	−12.326	0.0103	1.416	0.978	−19.955	0.0814	1.417	0.978	−20.011	0.0820
H	1.138	1.025	−12.326	0.0101	1.408	0.978	−19.993	0.0810	1.364	0.981	−19.173	0.0718
C_4	0.962	0.999	−17.003	0.0088	1.234	0.954	−26.478	0.0672	1.265	0.953	−26.963	0.0768
					VS of C_4							
C_3	0.971	0.998	−17.389	0.0067	0.823	1.045	−10.305	0.0704	0.845	1.044	−10.336	0.0672
H	1.132	1.026	−12.293	0.0088	1.165	1.014	−13.859	0.0218	1.169	1.014	−13.906	0.0237
H	1.132	1.026	−12.293	0.0088	1.226	1.009	−14.790	0.0391	1.208	1.012	−14.291	0.0414
H	1.138	1.025	−12.470	0.0096	1.216	1.010	−14.561	0.0410	1.219	1.010	−14.617	0.0412

[a] Calculated using HF/6-311++G**.r_c is the distance from the (3, −3) CP to the carbon nuclei, in au. All quantities are in atomic units, and ϵ is dimensionless. The symbols are explained in the text.

n-butane molecule. In Table 1 we show the properties of the CPs of charge concentration at the valence shell (VSCC) of the carbon atoms corresponding to the *n*-butane molecule and the two isomers that result from the protonation of the C_2-C_3 bond, structures **10** and **11** (see Figure 1). The *n*-butane molecule analysis will be used as a reference for the study of all the protonated species. The reported values for each carbon atom are as follows: the Laplacian in the (3, −3) CPs, $-\nabla^2\rho$; the distance from the CP to the carbon nuclei, r_c; the perpendicular curvature to the surface of the sphere of charge concentration or radial curvature, λ_3; and the ellipticity defined by the relationship between the two tangential curvatures, λ_1 and λ_2, $\epsilon = (\lambda_1/\lambda_2) - 1$.

In the *n*-butane molecule, the valence shell of each carbon atom, VS, exhibits four local maxima in $-\nabla^2\rho$, which are located at the direction of each C−C or C−H bond (bond path). That makes a total of 16 (3, −3) CPs. The C_1 and C_4 and C_2 and C_3 carbon atoms are topologically equivalent due to the molecular geometry (the values of $-\nabla^2\rho$, r_c, λ_3, and ϵ in the (3, −3) CPs are similar). The CPs that are located at the C−C bond path show lower values of $-\nabla^2\rho$ and r_c and higher values of λ_3 than the CPs localized at the C−H bond path. These parameters show a small difference regarding primary and secondary carbon atoms.

We present in Figure 2 the relief map of the *n*-butane molecule in the plane of all the carbon atoms. At their extremes there are two maxima corresponding to the position of the hydrogen atoms. Also, we can see at the position of each carbon atom the core and valence shell charge concentration. In the C−C bond path, the two (3, −3) CPs corresponding to each valence shell of a carbon atom are highly symmetrical. Also, there are other (3, −3) CPs corresponding to the C−H bonds located at the C_4-H and C_1-H bond paths.

When the parameters obtained at the CPs on the VS of the carbon atoms in the two isomers of 2-*C*-*n*-butonium (structures **10** and **11**, see Table 1) are analyzed, the loss of the symmetry found in the C−C regions of the *n*-butane molecule can be clearly seen ($-\nabla^2\rho = 0.971$ au and 0.962 au in *n*-butane and $\nabla^2\rho = 0.847$ au and 1.263 au, respectively, in isomer **10**).

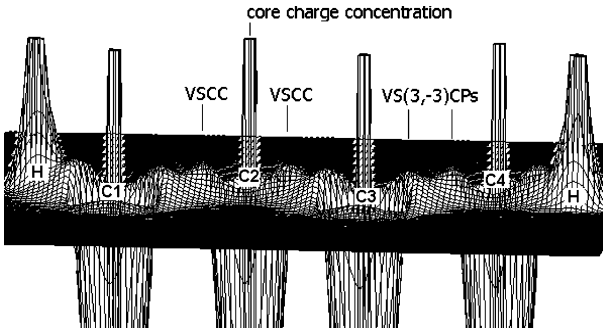

Figure 2. Relief map of the Laplacian distribution in *n*-butane molecule, in the plane of the carbons atoms. At their extremes there are two maxima corresponding to the position of the hydrogen atoms. In the C−C bond path, the two CPs corresponding to each VS of a carbon atom are highly symmetrical. Also, there are other (3, −3) CPs corresponding to the C−H bonds located at the C_4-H and C_1-H bond paths.

The CPs corresponding to the valence shell of the C_2 and C_3 atoms at the C−C bond region are displaced slightly approaching the nuclei (r_c decreases ≈ 0.050 au), and there is an increase of about 20% in the values of the Laplacian. The parameter λ_3 shows more significant changes during the protonation process, and the modifications of the other two curvatures produce an increase of 1 order of magnitude in the ellipticity values. Similar changes, although of a minor magnitude, are observed on the VS of the C_1 and C_4 atoms in the C−H bond paths. However, at the VS of C_1 in the CP on the C_1-C_2 bond path the values of the Laplacian decrease from 0.971 to 0.847−0.844 au and λ_3 decreases from −17.390 au to −10.418 au and −10.335 au in structures **10** and **11**, respectively. Their ellipticity values, although near zero, increase more than in the C−H CPs. Besides, these CPs move away from the C_1 atom (r_c increases 0.06 au). Therefore, the topological characteristics of the Laplacian of ρ show how the accumulation of the charge density at the C_1-C_2 bond region (near C_1) is dispersed (it is flattened), and it is moved, like the C−H PCs, toward the site involved at the three-center-two-electron bond. Similar considerations can be done for the CP localized in the VS of the C_4 atom in the C_3-C_4

TABLE 2: Topological Local Properties at the (3, −3) CPs of $-\nabla^2\rho_{(r_c)}$ in the Valence Shell of the Carbon Atoms in 1-*C*-*n*-Butonium[a]

	7			**9**				**8**			
	$-\nabla^2\rho(r)$	λ_3	ϵ	$-\nabla^2\rho(r)$	r_c	λ_3	ϵ	$-\nabla^2\rho(r)$	r_c	λ_3	ϵ
					VS of C_1						
H	1.371	−19.043	0.0634	1.372	0.983	−19.125	0.0640	1.372	0.983	−19.108	0.0643
H	1.373	−19.045	0.0633	1.375	0.983	−19.061	0.0629	1.376	0.983	−19.103	0.0633
H	1.313	−18.069	0.0492	1.321	0.987	−18.219	0.0540	1.317	0.987	−18.171	0.0519
H*											
					VS of C_2						
H*											
H	1.435	−20.858	0.1034	1.450	0.972	−21.192	0.1028	1.440	0.973	−20.924	0.1060
H	1.459	−21.262	0.1004	1.452	0.973	−21.059	0.1016	1.453	0.973	−21.060	0.1035
C_3	1.312	−29.142	0.0838	1.302	0.945	−29.009	0.0832	1.307	0.944	−29.197	0.0932
					VS of C_3						
C_2	0.809	−9.423	0.0856	0.800	1.052	−9.395	0.0887	0.803	1.052	−9.332	0.0745
H	1.227	−14.757	0.0431	1.157	1.016	−13.583	0.0182	1.233	1.008	−14.798	0.0359
H	1.158	−13.625	0.0194	1.234	1.007	−14.923	0.0425	1.235	1.008	−14.828	0.0352
C_4	1.058	−20.642	0.0506	1.057	0.981	−20.651	0.0516	0.988	0.803	−19.822	0.0274
					VS of C_4						
C_3	0.874	−13.608	0.0125	0.872	1.022	−13.574	0.0151	0.803	1.029	−12.720	0.0269
H	1.211	−14.582	0.0204	1.211	1.010	−14.583	0.0207	1.203	1.010	−14.509	0.0194
H	1.138	−12.498	0.0282	1.171	1.019	−13.304	0.0272	1.186	1.016	−13.698	0.0304
H	1.174	−13.415	0.0269	1.144	1.024	−12.624	0.0286	1.184	1.016	−13.646	0.0297

[a] Calculated using HF/6-311++G**.r_c is the distance from the (3, −3) CP to the carbon nuclei, in au. All quantities are in atomic units, and ϵ is dimensionless. The symbols are explained in the text.

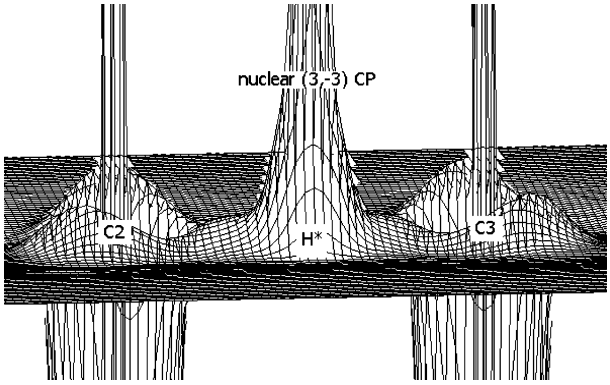

Figure 3. Relief map of the Laplacian distribution in compound **11** (2-*C*-*n*-butonium) in the plane that contains the $C_2-H^*-C_3$ atoms. The nuclear CP of H* in the region of the three-center bond can be seen. Comparison with Figure 2, at the VS of C_2 and C_3 in *n*-butane, allows one to see how the VS (3, −3) CPs existing in the C_2-C_3 bond region are lost in the protonated species. It is worth noting the flatness of the Laplacian distribution at the bonding C−H* regions.

bond path. Consequently, very different characteristics are observed in the two CPs found in the C−C bonds. The CPs of the larger Laplacian values, λ_3 and ϵ, are those belonging to the VS of the C atoms involved in the 3c-2e bonds, $C_{(H^*)}$. These are located at a smaller distance of the nuclei of $C_{(H^*)}$. It has to be remarked that the values of the Laplacian are larger than the values corresponding to the (3, −3) CPs localized in the bonding region between the C and H atoms in the *n*-butane molecule ($\approx$ 1.26 au vs 1.13 au), and also the values are larger than those found in the C−H bond region of the carbon atoms adjacent to the protonated ones.

The most notable characteristic of the Laplacian of ρ distribution is observed in the region of the 3c-2e bond. We present in Figure 3 the relief map of the distribution in the plane containing the $C_2-H^*-C_3$ atoms. A maximum, also a (3, −3) CP, is observed at the H* nucleus position. This kind of CP will be named a "nuclear CP" (it shows a Laplacian value an order of magnitude higher and a similarly higher perpendicular curvature (λ_3) than the VS CPs) and will be topologically analyzed below. The comparison of the appearance of the relief map at the zone of C_2 and C_3 in *n*-butane allows one to see how the VS (3, −3) CPs existing in the C_2-C_3 bond region are lost in the protonated species. It is worth noting the flatness of the Laplacian distribution at the bonding C−H* regions.

We report in Table 2 the properties of the CPs over the VS of the carbon atoms corresponding to the three isomers that result from the protonation of the C_1-C_2 bond (see Figure 1) in compounds **7**, **8**, and **9**. We found for the protonation region similar values as those in 2-*C*-*n*-butane. On the VS of the C_1 and C_2 atoms, the CPs approach the nuclei (r_c decreases), the value of the Laplacian and the curvature λ_3 increase, and the ellipticity values, although near zero, are larger by 1 order of magnitude. The same happens in the CPs of the C_3-H and C_4-H bond regions and on the VS of the C_3 atom only in the C_3-C_4 bond path. The CPs on the VS of the C_3 and C_4 atoms in the C_2-C_3 and C_3-C_4 bond paths, respectively, move away from these carbon nuclei (r_c increases), and also there is a decrease of the Laplacian and λ_3 values. The movements of the CPs with respect to the nuclei position, both when r_c is increasing or when it is decreasing, show how the CPs are carried out toward the protonation site. This finding, like in 2-*C*-*n*-butonium, indicates a displacement effect of the electronic charge density through the sigma bonds. Here again, the value of the Laplacian corresponding to the (3, −3) CP in the VS of the C(H*) in the region between the carbon atoms is larger than the value found in the C−H bond region of the carbon atoms adjacent to the protonated one and in CH bonds in the *n*-butane molecule.

In the 1-*C*-*n*-butonium, as well as in the 2-*C*-*n*-butonium cations, no CPs at the valence shell are found in the region of the three-center-two-electron bond $C_1-H^*-C_2$. These features can be seen in Figure 4 where we show a relief map of isomer **8** in the plane of $C_3-C_2-H^*$. C_1 is slightly out of plane, and the absence of the CPs previously found between C_1 and C_2 in the *n*-butane molecule can be seen. There it is easy to distinguish the nuclear (3, −3) CP at the H* position, and the flatness of the Laplacian distribution at the C−H* regions can also be noted. Moreover, on each C−C region it is possible to appreciate

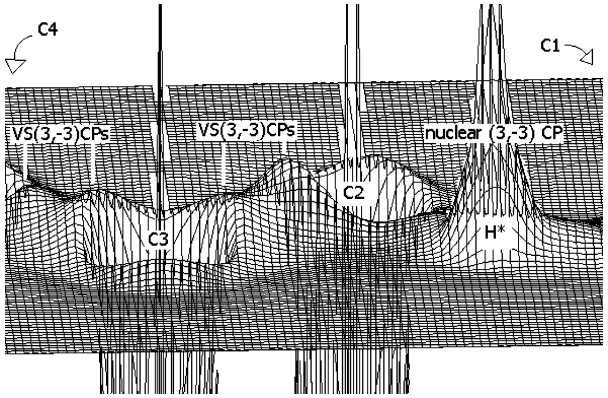

Figure 4. Relief map of the Laplacian distribution in compound **8** (1-*C*-*n*-butonium) in the plane that contains the C_2-C_3 bond; C_1 is slightly out of plane. The asymmetry of the two maxima located at the direction of this bond can be noted, and it is possible to appreciate how the highest maxima are always closer to the protonation zone. The presence of the charge concentration CP at the H* atom and the absence of the charge concentration CP at the VS of C(H*) on the C−H* bond directions can be observed. The flatness of the Laplacian distribution at the C−H* regions can also be noted.

how the highest $-\nabla^2\rho$ values at the VS (3, −3) CPs are always closer to the protonation zone. A CP of the highest λ_3 value is found on the VS of C_2 in the C_2-C_3 bond path (although not with a higher Laplacian value; $\lambda_3 = -29.142$ and $-\nabla^2\rho = 1.312$ au), which denotes a charge concentration very acute and next to C_2 in the bonding region. The other CP existing in this bond path in the VS of C_3 shows very different characteristics as a result of the electronic redistribution that operates upon protonation. It is easy to note in Figure 4 the asymmetry among both (3, −3) CPs located on the C_2-C_3 bond. The trend observed is similar to that explained above in 2-*C*-*n*-butane. The same characteristics are found in the C_3-C_4 bond although they are somewhat smaller.

Figure 5a displays the relief map of the Laplacian distribution, in the plane that contains the carbon and hydrogen atoms involved at the three-center-two-electron bond, C_2-H^*-H, in isomer **4**. This corresponds to the species 2-*H*-*n*-butonium, and there are two symmetrical maxima. They are centered at the position of the involved hydrogen atoms and correspond also to nuclear CPs. This can be qualitatively observed also in other relief maps (see Figures 3 and 4). Moreover, the absence of a CP (3, −3) on the valence shell of the C_2 atom, in the direction of these hydrogen atoms, is noted. In the valence shell of the C_2 atom, in the direction of the C_1 atom (C_1 is out of the plane), there is a CP (3, −3). The relief map of the Laplacian distribution for the H−H* bond is topologically similar to that observed for the isolated H_2 molecule, at the same level of calculation (see Figure 5b).

We display in Table 3 the properties of the CPs on the VS of the carbon atoms corresponding to the three isomers that result from the protonation of the C_2-H bond (see Figure 1), compounds **4**, **5**, and **6**. It is found that the distribution is fundamentally modified in the valence shell of the C_2 atom. The (3, −3) CP approach the nuclei (r_c decreases) and the Laplacian and curvatures values increase, and this change is more evident in the λ_3 and ϵ values for the CPs localized in the C_2-C_1 and C_2-C_3 bond paths. These maxima of electronic charge concentration are more acute ($\lambda_3 = -26.785$ au and −27.641 au), and they approach 0.05 au at the C_2 atom, involved in the 3c-2e interaction.

When compared with *n*-butane, the same number of (3, −3) CPs are found in the valence shells of the other carbon atoms,

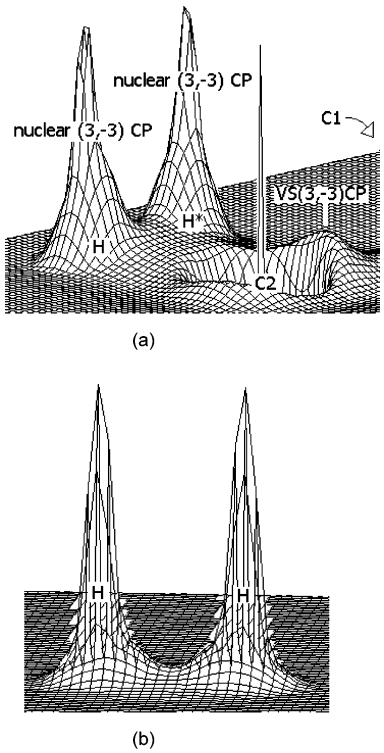

Figure 5. (a) Relief map of the Laplacian distribution in compound **4** (2-*H*-*n*-butonium) in the plane that contains the carbon and hydrogen atoms involved at the three-center-two-electron bond, C_2-H^*-H. There are two symmetrical maxima which are centered at the position of the involved hydrogen atoms. The absence of a CP (3, −3) on the valence shell of the C_2 atom, in the direction of these hydrogen atoms, and the flatness of the distribution at the region of the C−H* bond can be noted. In the valence shell of the C_2 atom, in the direction of the C_1 atom (C_1 is out of the plane), there is a CP (3, −3). (b) The relief map of the Laplacian distribution for the H−H* bond is similar to that observed for the isolated H_2 molecule, at the same level of calculation.

but also with some differences in their topological characteristics. The analysis of variations in the r_c values of the CPs as well as the other characteristics (variations found in ϵ, λ_3, and $-\nabla^2\rho$ values) indicates (as in the previous species) that the electronic density delocalizes through the sigma bonds C−C and C−H of the molecule toward the region of highest requirements of electronic density, which in our case is the protonation site.

Similar considerations can be done from the analysis of the results shown in Table 4 for the 1-*H*-*n*-butonium cations. In this molecular species the protonation occurs on the C_1-H bond, and it can be seen how the CP (3, −3) of the VS of C_1 localized in the direction of the sigma bond of the carbonated chain shows an approach and a much more acute form than the other VS CPs existing both in this type of molecule and in *n*-butane (i.e., $\lambda_3 = -28.400$ in structure **2**). This feature can be observed qualitatively in Figure 6, where a relief of the Laplacian map corresponding to the C_2-C_1-H plane is displayed. In this figure it is also possible to see the (3, −3) CP at the two terminal hydrogen atoms placed approximately in the same plane; over them are localized the nuclear CPs. At the valence shell of C_1 and C_4, in the corresponding C−H bond region, are observed the typical (3, −3) CPs. The difference between the two kinds of (3, −3) CPs, nuclear and VSCC, can be easily seen. This can be qualitatively noted also in other relief maps (see Figures 4 and 5a).

The displacements encountered in all other CPs follow the patterns found in the previously analyzed species, that is, in

TABLE 3: Topological Local Properties at the (3, −3) CPs of $-\nabla^2\rho_{(r_c)}$ in the Valence Shell of the Carbon Atoms in 2-*H*-*n*-Butonium[a]

	5				6				4			
	$-\nabla^2\rho(r)$	r_c	λ_3	ϵ	$-\nabla^2\rho(r)$	r_c	λ_3	ϵ	$-\nabla^2\rho(r)$	r_c	λ_3	ϵ
					VS of C_1							
H	1.221	1.009	−14.745	0.0405	1.220	1.009	−14.690	0.0388	1.220	1.009	−14.671	0.0405
H	1.216	1.008	−14.796	0.0333	1.210	1.009	−14.652	0.0324	1.219	1.008	−14.828	0.0320
H	1.228	1.008	−14.834	0.0432	1.231	1.008	−14.859	0.0415	1.215	1.010	−14.527	0.0423
C_2	0.768	1.053	−9.554	0.0495	0.774	1.052	−9.674	0.0482	0.784	1.051	−9.829	0.0467
					VS of C_2							
C_1	1.214	0.954	−26.785	0.1037	1.214	0.954	−26.674	0.1044	1.212	0.955	−26.427	0.1000
H	1.229	0.998	−16.103	0.0701	1.247	0.996	−16.542	0.0744	1.324	0.987	−18.167	0.1096
H*H′												
C_3	1.210	0.950	−27.641	0.1303	1.208	0.950	−27.638	0.1176	1.075	0.959	−25.394	0.0999
					VS of C_3							
C_2	0.725	1.059	−9.050	0.0557	0.719	1.059	−9.000	0.0544	0.627	1.068	−8.352	0.0694
H	1.226	1.007	−14.881	0.0294	1.226	1.007	−14.935	0.0330	1.249	1.005	−15.274	0.0423
H	1.235	1.007	−14.873	0.0423	1.231	1.008	−14.825	0.0427	1.250	1.004	−15.344	0.0448
C_4	1.058	0.981	−20.673	0.0494	1.061	0.980	−20.750	0.0508	1.071	0.974	−21.932	0.0419
					VS of C_4							
C_3	0.873	1.021	−13.634	0.0200	0.877	1.021	−13.717	0.0169	0.828	1.030	−12.477	0.0241
H	1.211	1.009	−14.647	0.0208	1.210	1.010	−14.579	0.0192	1.206	1.010	−14.485	0.0230
H	1.170	1.019	−13.283	0.0296	1.127	1.027	−12.203	0.0282	1.194	1.015	−13.831	0.0325
H	1.141	1.025	−12.527	0.0308	1.183	1.017	−13.587	0.0287	1.179	1.017	−13.496	0.0312

[a] Calculated using HF/6-311++G**.r_c is the distance from the (3, −3) CP to the carbon nuclei, in au. All quantities are in atomic units, and ϵ is dimensionless. The symbols are explained in the text.

TABLE 4: Topological Local Properties at the (3, −3) CPs of $-\nabla^2\rho_{(r_c)}$ in the Valence Shell of the Carbon Atoms in 1-*H*-*n*-Butonium[a]

	2				1				3			
	$-\nabla^2\rho(r)$	r_c	λ_3	ϵ	$-\nabla^2\rho(r)$	r_c	λ_3	ϵ	$-\nabla^2\rho(r)$	r_c	λ_3	ϵ
					VS of C_1							
H	1.315	0.986	−18.460	0.1048	1.340	0.984	−18.790	0.0943	1.335	0.986	−18.567	0.0969
H	1.166	1.004	−15.200	0.0481	1.168	1.004	−15.199	0.1039	1.335	0.986	−18.490	0.0968
H*H′												
C_2	1.225	0.948	−28.400	0.0776	1.196	0.949	−28.142	0.1184	0.975	0.965	−24.230	0.0093
					VS of C_2							
C_1	0.701	1.069	−7.998	0.0353	0.672	1.073	−7.700	0.0471	0.514	1.093	−6.444	0.086
H	1.238	1.007	−14.986	0.0473	1.235	1.007	−14.921	0.0478	1.275	0.999	−16.125	0.0581
H	1.228	1.007	−14.981	0.0390	1.245	1.006	−15.143	0.0495	1.275	0.997	−16.414	0.0476
C_3	1.087	0.975	−21.795	0.0650	1.093	0.972	−22.506	0.0589	1.139	0.967	−23.447	0.0727
					VS of C_3							
C_2	0.866	1.022	−13.423	0.0074	0.835	1.028	−12.636	0.0086	0.86	1.027	−12.784	0.0120
H	1.169	1.020	−13.122	0.0201	1.180	1.017	−13.386	0.0227	1.187	1.016	−13.574	0.0211
H	1.139	1.025	−12.342	0.0220	1.174	1.019	−13.214	0.0219	1.136	1.025	−12.296	0.0229
C_4	1.042	0.982	−20.332	0.0249	1.037	0.983	−20.088	0.0267	1.044	0.981	−20.437	0.0247
					VS of C_4							
C_3	0.876	1.019	−13.954	0.0039	0.883	1.018	−14.181	0.0062	0.869	1.021	−13.754	0.0060
H	1.191	1.014	−13.920	0.0208	1.189	1.014	−13.903	0.0193	1.194	1.013	−14.040	0.0210
H	1.165	1.020	−13.134	0.0234	1.163	1.021	−13.061	0.0228	1.167	1.020	−13.185	0.0245
H	1.168	1.019	−13.208	0.0232	1.163	1.020	−13.082	0.0230	1.168	1.019	−13.241	0.0243

[a] Calculated using HF/6-311++G**.r_c is the distance from the (3, −3) CP to the carbon nuclei, in au. All quantities are in atomic units, and ϵ is dimensionless. The symbols are explained in the text.

these carbocationic species the electronic charge delocalizes through sigma bonds. We present graphically in Figure 7 the displacements experienced by each VSCC CP with respect to *n*-butane taking as an example one isomer of each molecular species.

As in the all other cases, a decrease in the distance of their (3, −3) CPs to the nuclei at the VS of the C(H*) and an increase of the Laplacian function and the λ_3 values is found. It can be interpreted that an atom deficient in electrons (more electronegative carbon atom) results in an attractor of the molecular electronic density, and so the local maxima found in its valence shell show higher Laplacian and radial curvature values. These data can be related to the local values of the potential energy (everywhere negative) and the kinetic energy (everywhere positive) following the local statement of the Virial theorem:

$$h^2/4m\nabla^2\rho = 2\,T(r) + V(r)$$

where $T(r)$ and $V(r)$ represent the kinetic and potential energy densities. And so whenever the $\nabla^2\rho$ results are negative it means the potential energy is the dominant one which is the case of one (3, −3) CP.

On the other hand, the density of the total electronic energy function is related to the density of the potential and kinetic energy by the expression

$$E_e(r) = T(r) + V(r)$$

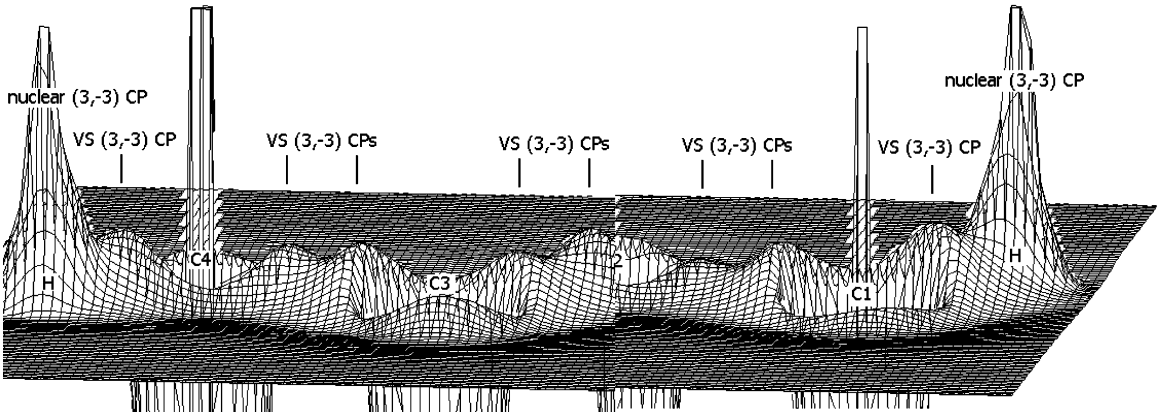

Figure 6. Relief map of the Laplacian distribution in compound **3** (1-*H*-*n*-butonium) in the C_2-C_1-H plane. There are two terminal hydrogen atoms placed approximately in the same plane; over them are localized the charge concentration points. At the VS of C_1 and C_4, in the corresponding C−H bond region, are shown the typical (3, −3) CPs. The difference between the two kinds of (3, −3) CPs, nuclear and VSCC, besides the asymmetry of the (3, −3) CPs on the C−C bonds can be seen. The H* atom is out of plane.

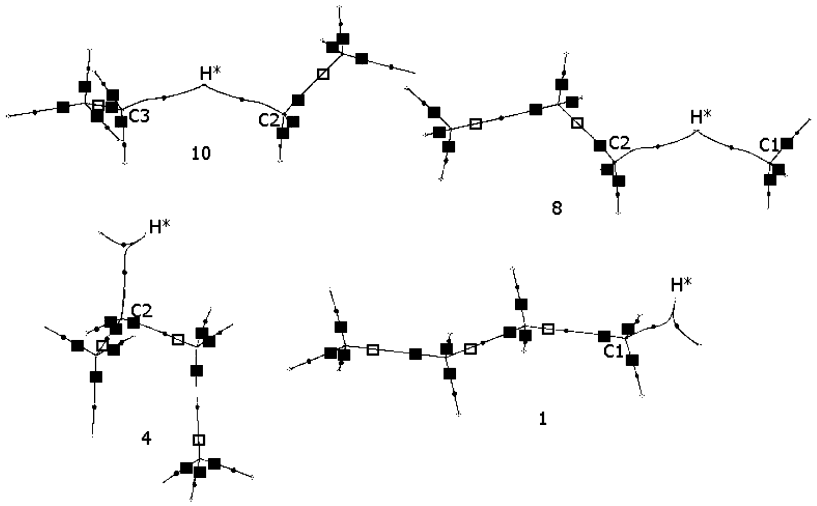

Figure 7. Molecular graphs of the different species (2-*C*-, 1-*C*-, 2-*H*-, and 1-*H*-*n*-butonium). The location of the VS (3, −3) CPs of the Laplacian of electronic density are indicated approximately on the VS of each carbon atom. Empty (filled) squares indicat the CPs that go away from (come closer to) the carbon atom. The bond critical points (obtained form topological analysis of the electronic density) are denoted by filled circles.

TABLE 5: Values of the Kinetic, Potential, and Total Electronic Energy Densities ($T(r)$, $V(r)$, and $E_e(r)$ Respectively) for the (3, −3) CPs at the VS of C(H*) in 2-*C*-*n*-Butonium and 2-*H*-*n*-Butonium[a]

	2-*C*-*n*-butonium			2-*H*-*n*-butonium		
	C	H	H	C	C	H
$T(r)$	0.1563	0.1279	0.1263	0.1579	0.1623	0.1307
$-V(r)$	0.6289	0.5967	0.6069	0.6187	0.5932	0.5924
$-E_e(r)$	0.4726	0.4688	0.4806	0.4608	0.4309	0.4617

[a] Following the location of the CPs, they are reported according to the C(H*)−X bond path (see Figures 3 and 5a). Only one isomer of each molecular species is shown. Wave functions at the HF/6-311++G** level. All values are expressed in au.

where $E_e(r)$ designates the density of the local total electronic energy. We report in Table 5 the values of $T(r)$, $V(r)$, and $E_e(r)$ for the (3, −3) CPs at the VS of C(H*) in 2-*C*-*n*-butonium and 2-*H*-*n*-butonium. Only one isomer of each molecular species is shown. It can be seen that the higher Laplacian values result from an increase of V(r). The relative stability of 2-*C*-*n*-butane with respect to the other species is related to higher values of local potential and total electronic energy densities, although the kinetic energy density changes more slightly.

A 2-*C*-*n*-butonium cation shows the highest values of $-\nabla^2\rho$ in the three (3, −3) CPs of both the C_2 and C_3 atoms, indicating a local gain of $V(r)$ and $G(r)$ in the environment of the secondary carbon atoms. On its turn, it confers to this species a higher stability (in Table 5 only the VS CPs of one carbon are displayed). Similar findings correspond to 1-*C*-*n*-butonium. In the 2-*H*- and 1-*H*-*n*-butonium cations the CPs around the primary or secondary carbon atoms show only three CPs where the Laplacian shows higher values, and consequently the local increase of the potential and electronic energy density is smaller.

In addition, we also analyze the (3, −3) and (3, +3) CPs around the hydrogen positions. A study of charge concentration over the hydrogen nuclei (as was seen above) can be done by analyzing the corresponding (3, −3) CP which appears centered at the nuclear coordinates. Besides, a (3, +3) CP is found for each H atom. This CP is located at the corresponding C−H bond path but at the nonbonding region and located approximately to 0.7 au away from the nuclei. In the *n*-butane molecule these points are always more far apart from the hydrogen nuclei (0.775−0.779 au) than in the protonated compounds (i.e., 0.750−0.762 au in isomer **10**). Also, an increase in the depth (the value of the $-\nabla^2\rho$) of the (3, +3) CPs (Laplacian values between 0.103 and 0.107 au and 0.117−0.131 au in the neutral species and isomer **10**, respectively) is found. The increase in the depth is always related to the decrease of $-\nabla^2\rho$ at the (3, −3) nuclear CP, that is, the increase of charge depletion near the hydrogen atom is accompanied by the decrease of charge concentration over the nuclear position.

TABLE 6: Local Properties at (3, +3) and (3, −3) of $-\nabla^2\rho_{(r_c)}$ CPs over the Atoms of H* [a]

		(3, +3)					(3, −3)				
	r_c	$-\nabla^2\rho(r)$	λ_1	λ_2	λ_3	ϵ	$-\nabla^2\rho(r)$	λ_1	λ_2	λ_3	ϵ
3	0.721	−0.1466	0.076	0.107	4.211	−0.975	20.410	−2102.8	−2094.5	−2085.3	0.0044
1	0.725	−0.1416	0.092	0.118	4.204	−0.972	21.235	−2185.6	−2177.7	−2167.8	0.0046
2	0.726	−0.1399	0.089	0.115	4.156	−0.972	21.211	−2182.6	−2174.7	−2164.8	0.0046
4	0.726	−0.1453	0.080	0.105	4.163	−0.975	21.167	−2180.0	−2171.1	−2161.9	0.0043
6	0.729	−0.1422	0.091	0.113	4.112	−0.973	21.765	−2239.6	−2231.2	−2221.2	0.0045
5	0.729	−0.1424	0.092	0.118	4.142	−0.972	21.889	−2251.9	−2243.2	−2233.5	0.0043
8	0.775	−0.1404	0.096	0.157	2.978	−0.947	25.748	−2641.4	−2634.5	−2623.3	0.0043
9	0.778	−0.1398	0.095	0.155	2.865	−0.946	25.776	−2643.6	−2636.8	−2625.4	0.0044
7	0.775	−0.1407	0.096	0.151	2.957	−0.949	25.690	−2634.9	−2627.9	−2616.9	0.0042
11	0.796	−0.1285	0.075	0.146	2.282	−0.936	26.295	−2695.5	−2689.5	−2676.3	0.0050
10	0.807	−0.1268	0.075	0.150	1.976	−0.924	26.585	−2724.7	−2719.5	−2704.7	0.0055

[a] Calculated using HF/6-311++G**.r_c is the distance from the (3, −3) CP to the carbon nuclei, in au. All quantities are in atomic units, and ϵ is dimensionless. The symbols are explained in the text. The topological properties in the (3, −3) CP localized over a H-bond, at C_2 in structure 10, is taken as reference. (These values are $-\nabla^2\rho(r)$, −25.229 au; λ_1, −2579.5 au; λ_2, −2579.4 au; λ_3, −2557.1 au; ϵ, 0.0087.)

Therefore, it is interesting to analyze the characteristics of both charge depletion, CD, and charge concentration, CC, critical points at the H* atom. We present in Table 6 the topological characteristics of the (3, +3) CPs encountered over the nuclei position of the H*. It is found that the value of the $-\nabla^2\rho$ and the curvature λ_3, in this CP, decrease in the order 1-*C*-*n*-butonium > 2-*C*-*n*-butonium, and the distance with respect to the position of the H* nuclei increases (it changes from 0.721 au in compound **3** to 0.807 au in compound **10**). It is also worth remarking that the (3, +3) CPs on the hydrogen atoms of the *n*-butane molecule and those far apart from the protonation region in the charged species have a minimum ellipticity value ($\epsilon \approx -0.01$), while for the H* atoms we find ellipticity values ranging from −0.949 to −0.924 (in the *C*-*n*-butonium cations) and from −0.975 to −0.972 (in the *H*-*n*-butonium cations), respectively.

We also analyze in Table 6 the (3, −3) CPs found at the position of the H* nuclei. As we have mentioned before, the nuclear (3, −3) CPs have a Laplacian value an order of magnitude higher than the VSCC or (3, −3) CPs, and they correspond to the electronic charge concentration over the respective hydrogen nuclei (see Figure 6). These results are consistent with the basicity scale proposed by Esteves et al.[9b] where the major stability of the *C*-carbonium ions in front of the *H*-carbonium has been rationalized on the basis of the canonical structures for the 3c-2e bond, as shown in Scheme 2. In the case of the *H*-carbonium ions (R═H), there is only one resonance structure where the positive charge lies over the carbon atom of the alkyl group, while in *C*-carbonium there are two structures, indicating that less charge is concentrated on the over the H* in the *C*-carbonium ions. Concordantly, the values of the concentration of the electronic charge density over the H* in *C*-carbonium are about 25% higher than in the *H*-carboniums, as can be seen in Table 6, resulting in a better stabilization.

The values of the $-\nabla^2\rho$ are 25.69−25.77 au when the protonation occurs over the $C_{prim}-C_{sec}$ bond and 26.29−26.58 au when the protonation occurs over $C_{sec}-C_{sec}$ bond, which reflects the contribution of the alkyl groups by the inductive effect at the electron deficient region.

Also, the higher values of the local potential and total electronic energy densities found for the 2-*C*-*n*-butonium isomers discussed above indicate the greater stability of *C*-*n*-butoniums in front of *H*-*n*-butoniums and are in line with the basicity scale proposed by Esteves et al.[11]

We see here, similar to other hydrogen atoms, that an increase of the charge concentration over the H* nuclei is related to a decrease in the depth of the charge depletion point.

Concluding Remarks

Due to the flatness of the Laplacian distribution at the bonding region involved in the 3c-2e interaction in all the studied protonated species, no (3, −3) CPs are found at the valence shell of C(H*), at least at this theoretical level. However, one may note that, in relation to the *n*-butane molecule, the (3, −3) CPs corresponding to the VS of the C(H*) in these carbocations are displaced toward the nuclei; the values of the Laplacian, the perpendicular curvature, and the ellipticity are augmented. Similar changes, although of minor magnitude, are observed on the VS of the adjacent carbon atoms, in the C−H bond paths. Besides, an asymmetrical distribution is clearly observed on the C−C bonds, depending on the CP spatial localization in relation to the protonation site.

In addition, we must remark that the increment in the Laplacian values at C(H*) is accomplished by an increase of the local density of the potential and electronic energy at the protonated carbons.

The Laplacian values in the CPs of depletion of the charge density on the hydrogen atoms involved in the three-center bond decrease in the order:

2-*C*-*n*-butoniums < 1-*C*-*n*-butoniums < 2-*H*-*n*-butoniums < 1-*H*-*n*-butoniums

while the nuclear CPs show an opposite behavior. These results allow us to conclude that the highest stability is obtained when the electronic charge density delocalizes through the sigma bonds toward the protonation site and overlaps more efficiently the H* nuclei.

The analysis performed here shows that the Laplacian of the charge density is a sensitive probe to detect differential charge density delocalization in sigma bonds and also shows how it can be helpful for gaining a deep understanding of the relative stability of the studied species and how it can be employed in a complementary way with the analysis of the proper charge density. Finally, it is worth stressing that this theoretical study is based on a real physical property of the system, molecular orbital independent and without employing any arbitrary charge, and it is performed on species in which the experimental determinations of charge density are practically impossible, reinforcing the importance of performing this sort of study.

Major refinements in the analysis, using MP2 and different wave functions, are in progress in our laboratory, and the results will be presented elsewhere.

Acknowledgment. N.M.P., G.L.S., and R.M.L. thank the SECYT UNNE for financial support. A.H.J. is a member of the Scientific Research career of CICPBA, Argentina.

References and Notes

(1) Field, F. H.; Munson, M. S. B. *J. Am. Chem. Soc.* **1965**, *87*, 3289.

(2) Hiraoka, K.; Kebarle, P. *J. Am. Chem. Soc.* **1976**, *98*, 6119−6125.

(3) (a) Boo, D. W.; Lee, Y. T. *Chem. Phys. Lett.* **1993**, *211*, 358. (b) Boo, D. W.; Lee, Y. T. *J. Chem. Phys.* **1995**, *103*, 520. (c) Boo, D. W.; Liu, Z. F.; Suits, A. G.; Lee, Y. T. *Science* **1995**, *269*, 57. (d) Bunker, P. R. *J. Mol. Spectrosc.* **1996**, *176*, 297. (e) Boo, P. W.; Loe, Y. T. *Int. J. Mass. Spectrom. Ion Processes* **1996**, *159*, 209.

(4) (a) Yeh, L. I.; Price, J. M.; Lee, Y. T. *J. Am. Chem. Soc.* **1989**, *111*, 5597. (b) Obata, S.; Hirao, K. *Bull. Chem. Soc. Jpn.* **1993**, *66*, 3271.

(5) Carneiro, J. W. M.; Schleyer, P. v. R.; Saunders, M.; Remington, R.; Schaefer, H. F., III; Rauk, A.; Sorensen, T. S. *J. Am. Chem. Soc.* **1994**, *116*, 3483−3493.

(6) East, A. L. L.; Liu, Z. F.; McCague, C.; Cheng, K.; Tse, J. S. *J. Phys. Chem. A* **1998**, *108*, 10903.

(7) Esteves, P. M.; Mota, C. J. A.; Ramirez-Solis, A.; Hernandez-Lamoneda, R. *J. Am. Chem. Soc.* **1998**, *120*, 3213.

(8) Mota, C. J. A.; Esteves, P. M.; Ramírez-Solís, A.; Hernández-Lamoneda, R. *J. Am. Chem. Soc.* **1997**, *119*, 5193−5199.

(9) (a) Esteves, P. M.; Mota, C. J. A.; Ramírez-Solís, A.; Hernández-Lamoneda, R. *Top. Catal.* **1998**, *6* (1−4), 163−168. (b) Esteves, P. M.; Alberto, G. G. P.; Ramirez-Solís, A.; Mota, C. J. A. *J. Phys. Chem. A* **2000**, *104*, 6233.

(10) (a) Collins, S. J.; O'Malley, P. J. *Top. Catal.* **1998**, *6*, 151−161. (b) Collins, S. J.; O'Malley, P. J. *Chem. Phys. Lett.* **1994**, *228*, 246. (c) Collins, S. J.; O'Malley, P. J. *J. Chem. Soc., Faraday Trans.* **1996**, *92*, 4347.

(11) Esteves, P. M.; Alberto, G. G. P; Ramírez-Solís, A.; Mota, C. J. A. *J. Am. Chem. Soc.* **1999**, *121*, 7345−7348.

(12) (a) Olah, G. A.; Halpern, Y.; Shen, J.; Mo, Y. K. *J. Am. Chem. Soc.* **1973**, *95*, 4960−4970. (b) Olah, G. A. *Angew. Chem., Int. Ed. Engl.* **1973**, *12*, 173. (c) Olah, G. A.; Prakash, G. K. S.; Williams, R. E.; Field, L. D.; Wade, K. *Hypercarbon Chemistry*; Wiley: New York, 1987.

(13) (a) Okulik, N.; Peruchena, N. M.; Esteves, P. M.; Mota, C.; Jubert, A. H. *J. Phys. Chem. A* **1999**, *103*, 8491. (b) Okulik, N.; Peruchena, N. M.; Esteves, P. M.; Mota, C.; Jubert, A. H. *J. Phys. Chem. A* **2000**, *104*, 7586.

(14) Okulik, N.; Esteves, P. M.; Mota, C.; Jubert, A. H.; Peruchena, N. M. *J. Phys. Chem. A* **2002**, *106*, 1584−1595.

(15) Bader, R. F. W. *Atoms in Molecules. A Quantum Theory*; Oxford Science Publications: Clarendon Press: London, 1990.

(16) Popelier, P. L. A. *Atoms in Molecules. An Introduction*; Pearson Education: Harlow, UK, 2000.

(17) Bader, R. F. W.; Essén, H. *J. Chem. Phys.* **1984**, *80*, 1943.

(18) Popelier, P. L. A.; Bader, R. F. W. *Chem. Phys. Lett.* **1992**, *189*, 542.

(19) Caroll, M. T.; Bader, R. F. W. *Mol. Phys.* **1988**, *65*, 695.

(20) Koch, U.; Popelier, P. L. A. *J. Phys. Chem.* **1995**, *99*, 9747.

(21) Fidanza, N. G.; Suvire, F. D.; Sosa, G. L.; Lobayan, R. M.; Enriz, R. D.; Peruchena, N. M. *J. Mol. Struct. (THEOCHEM)* **2001**, *543*, 185.

(22) Caroll, M. T.; Chang, C.; Bader, R. F. W. *Mol. Phys.* **1988**, *63*, 387.

(23) Sosa, G. L.; Peruchena, N. M.; Contreras, R. H.; Castro, E. A. *J. Mol. Struct. (THEOCHEM)* **1997**, *401*, 77.

(24) Sosa, G. L.; Peruchena, N. M.; Contreras, R. H.; Castro, E. A. *J. Mol. Struct. (THEOCHEM)* **2002**, *577*, 219.

(25) Grimme, S. *J. Am. Chem. Soc.* **1996**, *118*, 1529.

(26) Bader, R. F. W.; Chang, C. *J. Phys. Chem.* **1989**, *93*, 2946.

(27) Bader, R. F. W.; MacDougall, P. J. *J. Am. Chem. Soc.* **1985**, *107*, 6788.

(28) Bader, R. F. W.; Chang, C. *J. Phys. Chem.* **1989**, *93*, 2946.

(29) Caroll, M. T.; Cheeseman, J. R.; Osman, R.; Weinstein, H. *J. Phys. Chem.* **1989**, *93*, 5120.

(30) Werstiuk, N. H.; Laidig, K. E.; Ma, J. *Application of Quantum Theory of Atoms in Molecules to Study of Anomeric Effect in Dimethoxymethane*; Thatcher, G. R. J., Ed.; ACS Symposium Series 539; American Chemical Society: Washington, DC, 1993.

(31) Bader, R. F. W.; Popelier, P. L. A.; Chang, C. *J. Mol. Struct. (THEOCHEM)* **1992**, *255*, 145.

(32) Niño, A.; Muñoz-Caro, C. *Biophys. Chem.* **2001**, *91*, 49.

(33) Sierraalta, A.; Ruette, F. *J. Mol. Catal. A: Chem.* **1996**, *109*, 227.

(34) Aray, Y.; Rodriguez, J.; Rivero, J.; Vega, D. *Surf. Sci.* **1999**, *441*, 344.

(35) Gillespie, R. J. *Struct. Chem.* **1998**, *9*, 73.

(36) Gillespie, R. J. R. *Can. J. Chem.* **1992**, *70*, 742.

(37) Fradera, X.; Austen, M. A.; Bader, R. F. W. *J. Phys. Chem. A* **1999**, *103*, 304.

(38) Bytheway, I.; Gillespie, R. J.; Tang, T. H.; Bader, R. F. W. *Inorg. Chem.* **1995**, *34*, 2407.

(39) Gillespie, R. J.; Bytheway, I.; Dewitte, R. S.; Bader, R. F. W. *Inorg. Chem.* **1994**, *33*, 2115.

(40) Bader, R. F. W.; Gillespie, R. J.; Martin, R. J. *Chem. Phys. Lett.* **1998**, *290*, 488.

(41) Bytheway, I.; Popelier, P. L.; Gillespie, R. J. *Can. J. Chem.* **1996**, *74*, 1059.

(42) Bader, R. F. W.; Heard G. L. *J. Chem. Phys.* **1999**, *111*, 8789.

(43) Popelier, P. L. A. *Coord. Chem. Rev.* **2000**, *197*, 169.

(44) Malcolm, N. O. J.; Popelier, P. L. A. *J. Phys. Chem.* **2001**, *105*, 7638.

(45) (a) Coppens, P. *X-ray Charge Densities and Chemical Bonding*; Oxford University Press: New York, 1997. (b) Wilson, K. S. *Nat. Struct. Biol.* **1998**, *5*, 627−630.

(46) Koritsánszky, T.; Flaig, R.; Zobel, D.; Krane, H. G.; Morgenroth, W.; Luger, P. *Science* **1998**, *279*, 356.

(47) Frisch, M. J.; Trucks, G. W.; Schlegel, H. B.; Scuseria, G. E.; Robb, M. A.; Cheeseman, J. R.; Zakrzewski, V. G.; Montgomery, J. A., Jr.; Stratmann, R. E.; Burant, J. C.; Dapprich, S.; Millam, J. M.; Daniels, A. D.; Kudin, K. N.; Strain, M. C.; Farkas, O.; Tomasi, J.; Barone, V.; Cossi, M.; Cammi, R.; Mennucci, B.; Pomelli, C.; Adamo, C.; Clifford, S.; Ochterski, J.; Petersson, G. A.; Ayala, P. Y.; Cui, Q.; Morokuma, K.; Malick, D. K.; Rabuck, A. D.; Raghavachari, K.; Foresman, J. B.; Cioslowski, J.; Ortiz, J. V.; Stefanov, B. B.; Liu, G.; Liashenko, A.; Piskorz, P.; Komaromi, I.; Gomperts, R.; Martin, R. L.; Fox, D. J.; Keith, T.; Al-Laham, M. A.; Peng, C. Y.; Nanayakkara, A.; Gonzalez, C.; Challacombe, M.; Gill, P. M. W.; Johnson, B. G.; Chen, W.; Wong, M. W.; Andres, J. L.; Head-Gordon, M.; Replogle, E. S.; Pople, J. A. *Gaussian 98*, revision A.7; Gaussian, Inc.: Pittsburgh, PA, 1998.

(48) Blieger-König, F. W.; Bader, R. F. W.; Tang, T. H. *J. Comput. Chem.* **1982**, *3*, 317.

(49) Bader, R. F. W.; Johnson, S.; Tang, T. H.; Popelier, P. L. A. *J. Phys. Chem.* **1996**, *100*, 15398.